Effects of Long Rarefied Plasmas on Fast Electron Generation for FIREX-I Targets

H. Sakagami[1], T. Johzaki[2], A. Sunahara[3], H. Nagatomo[2]

[1]*Fundamental Physics Simulation Div., National Institute for Fusion Science, Toki, Japan*

[2]*Institute of Laser Engineering, Osaka University, Osaka, Japan*

[3]*Institute for Laser Technology, Osaka, Japan*

1. Introduction

The FIREX-I project aims to demonstrate that the imploded core could be heated up to the ignition temperature, 5 keV, and integrated experiments for FIREX-I, in which heating is combined with implosion, have just started at Osaka University. Efficient heating mechanisms and achievement of such high temperature have not been, however, clarified yet, and we have been promoting the Fast Ignition Integrated Interconnecting code (FI^3) project to boldly explore fast ignition frontiers [1-4]. An unavoidable pre-pulse that is accompanied by the heating laser in FIREX-I generates the low-density plasmas, which fill up an inside of the cone. A main pulse of the heating laser has to interact with these preformed plasmas and it is pointed out that it results in low coupling efficiency. To prevent the preformed plasmas from being generated by the pre-pulse, the inside of the cone is suggested to be filled up with rarefied gases, which are ionized by the pre-pulse and expected to completely absorb the energy of the pre-pulse before irradiating the cone wall. As another scheme, an aperture of the cone is suggested to be covered with an extremely thin film. The pre-pulse could be interrupted and absorbed by this film, and cannot irradiate the cone wall. For both proposed methods, the main pulse must propagate through very long rarefied plasmas. There have been, however, few researches using such long rarefied plasmas. Thus we have investigated effects of long rarefied plasmas on core heating with the use of FI^3.

2. Rarefied Plasma and Fast Electrons

First of all, to investigate fast electron generation with use of the 1D PIC code, we set up the heating laser to λ_L=1.06 μm, τ_{HMFW}=1 ps, I_L=10^{20} Wcm^{-2}, and the Au-cone tip to 500n_{cr}, real mass, Z=30, 10 μm flattop plasma. We place the CH foam plasma (10n_{cr}, A=6.5, Z=3.5, 50 μm thickness) in front of the Au cone tip to generate fast electrons and the CD plasma

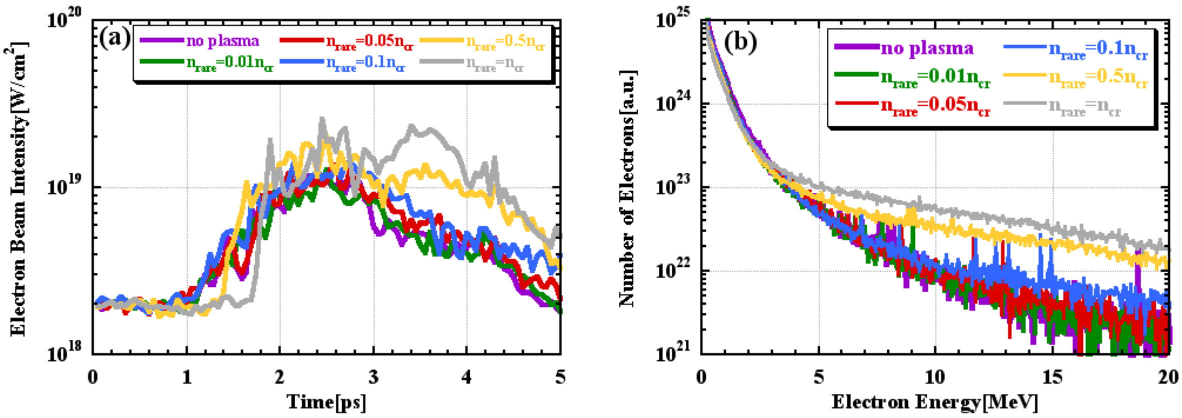

Fig.1 Fast electron properties with 150 μm thickness rarefied plasma. (a) time evolutions of fast electron beam intensity and (b) time averaged fast electron energy spectrum for n_{rare}=0, 0.01, 0.05, 0.1, 0.5 and 1n_{cr}.

(500n_{cr}, A=7, Z=3.5, 20 μm thickness) behind it as the compressed core. We also place the rarefied H plasma (0.01 ~ 1n_{cr}, A=1, Z=1, 150 or 300 μm thickness) in front of the CH foam.

Time evolutions of fast electron beam intensity and time averaged fast electron energy spectrum with n_{rare}=0, 0.01, 0.05, 0.1, 0.5, 1n_{cr} and 150 μm thickness are shown in Fig.1 (a) and Fig.1 (b), respectively. As the group velocity of the laser is slowing down in dense plasmas, rising time of the fast electron beam intensity is delayed longer with larger density of the rarefied plasma. When the density of the rarefied plasma is less than 0.1n_{cr}, both fast electron beam intensities and energy spectra are almost same as those in the case without the rarefied plasma. If the density is greater than 0.5n_{cr}, the laser-to-electron coupling efficiency increases because more laser energy is absorbed by the rarefied plasma, and the fast electron beam intensity becomes larger than that without the rarefied plasma. But this enhancement is mainly contributed by fast electrons with the energy more than 3 MeV, which are generated by interactions between the underdense rarefied plasma and the relativistic intensity laser and are not suitable for core heating.

Time evolutions of fast electron beam intensity and time averaged fast electron energy spectrum with same density but 300 μm thickness rarefied plasma are shown in Fig.2 (a) and Fig.2 (b), respectively. As the rarefied plasma is 150 μm longer than that in Fig.1, the time delay of rising of the beam intensity is expected to be 500 fs with the light speed and more duration for the rarefied plasma with larger density. When the rarefied plasma density is greater than 0.1n_{cr}, higher energy fast electrons are generated much more due to the longer rarefied plasma, and the fast electron beam intensity is also enhanced much more than that of the shorter rarefied plasma. But fast electrons with the energy less than 2 MeV are strongly

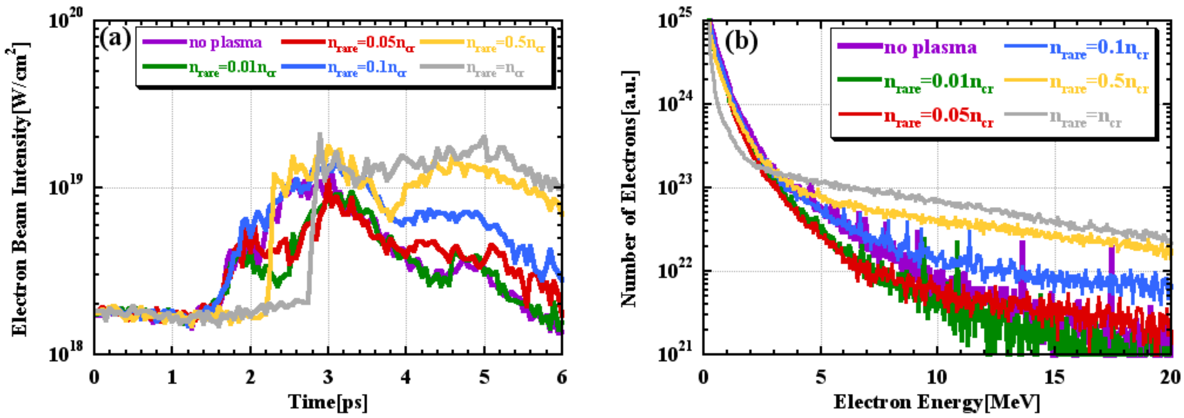

Fig.2 Fast electron properties with 300 μm thickness rarefied plasma. (a) time evolutions of fast electron beam intensity and (b) time averaged fast electron energy spectrum for n_{rare}=0, 0.01, 0.05, 0.1, 0.5 and $1n_{cr}$.

reduced in the case of $n_{rare}=n_{cr}$ because the laser intensity decreases before irradiating the CH foam plasma due to the large absorption rate and less fast electrons with lower energy can be generated. On the other hand, the fast electron beam intensity decreases than that without the rarefied plasma at $2 < t < 3$ ps in the cases of n_{rare}=0.01 and $0.05n_{cr}$. Electron density profiles around the laser-plasma interaction region for n_{rare}=0, 0.01, 0.05, $0.1n_{cr}$ and 300 μm thickness rarefied plasma at t=2.5 ps are shown in Fig.3. In the cases of n_{rare}=0 and $0.1n_{cr}$, the interaction region is filled with the critical density plasma and the profile steepening is reduced at the laser front. But there is no underdense plasma at the laser front and the CH form plasma is compressed to higher density than the initial density ($>10n_{cr}$) at the boundary, enhancing the profile steepening for the n_{rare}=0.01 and $0.05n_{cr}$ cases. This kind of electron steep density profile can substantially suppress the fast electron beam intensity to a low level [4].

3. Integrated Simulation for Core Heating

As the core heating is greatly affected by not only the beam intensity but also the energy spectrum of fast electrons, we have performed FI^3 integrated simulations to estimate core temperatures, assuming the same core parameters as in Ref.2. Maximum increments of the core electron temperature, which are averaged over the dense region (ρ>10 g/cm^3), and degradations against the

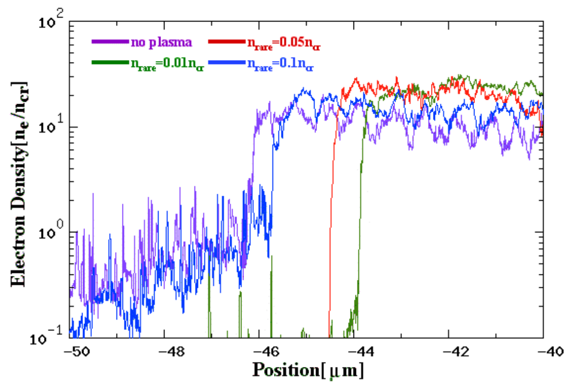

Fig.3 Electron density profiles around the laser-plasma interaction region for n_{rare}=0, 0.01, 0.05, $0.1n_{cr}$ and 300 μm thickness rarefied plasma at t=2.5 ps.

Table I. Maximum increments of the core electron temperature and degradations against the case without the rarefied plasma.

150 μm thickness						
n_{rare}/n_{cr}	0	0.01	0.05	0.1	0.5	1
increment [eV]	190	181	186	186	171	165
degradation[%]	-	4.4	1.9	2.0	9.8	13.0
300 μm thickness						
n_{rare}/n_{cr}	0	0.01	0.05	0.1	0.5	1
increment [eV]	182	159	155	181	156	82
degradation[%]	-	12.5	14.7	0.5	14.6	55.1

case without the rarefied plasma are summarized in Table I for n_{rare}=0, 0.01, 0.05, 0.1, 0.5, 1n_{cr} and 150, 300 μm thickness rarefied plasma.

In the case of 150 μm thickness rarefied plasma, fast electrons that are suitable for core heating (< 2 MeV) are not affected much by the rarefied plasma (*see Fig.1 (b)*) and the maximum core electron temperature is only reduced by 15 % even for the $n_{rare}=n_{cr}$ case. The degradation of temperature increment of the $n_{rare}=n_{cr}$ and 300 μm thickness case, however, reaches more than 50% because of much less appropriate fast electrons (*see Fig.2 (b)*).

According to 1D simulations including hydrodynamics and laser ray tracing, it is found that the 0.1 μm CH thin film which covers the cone aperture can be expanded to below 0.1n_{cr} after 1 ns by the pre-pulse with $I_L=10^{12}$ Wcm^{-2}. Thus this scheme is expected to reduce the pre-pulse level without the significant influence on the main laser.

Of course, the generation of fast electrons is simulated by 1D PIC code in this paper, multi-dimensional analyses including laser beam filamentation, diverging and merging in underdense plasma are needed to clarify our conclusion.

Acknowledgments

This work was supported by MEXT, Grant-in-Aid for Scientific Research (C)(22540511).

References

[1] H. Sakagami, et al., Laser Part. Beams **24**, 191-198 (2006).
[2] T. Johzaki, et al., Laser Part. Beams **25**, 621-629 (2007).
[3] H. Sakagami, et al., J. Phys.: Conf. Series **112**, 022070 (2008).
[4] H. Sakagami, et al., Nucl. Fusion **49**, 075026 (2009).